

PAPER • OPEN ACCESS

## Method for measuring the micro-discharges temperature in the micro-arc oxidation process

To cite this article: P E Golubkov *et al* 2019 *J. Phys.: Conf. Ser.* **1393** 012083

View the [article online](#) for updates and enhancements.



**IOP | ebooks™**

Bringing you innovative digital publishing with leading voices to create your essential collection of books in STEM research.

Start exploring the [collection](#) - download the first chapter of every title for free.

# Method for measuring the micro-discharges temperature in the micro-arc oxidation process

P E Golubkov, E A Pecherskaya, D V Artamonov and J V Shepeleva

Department of Information and measuring equipment and metrology Penza State University, 40 Krasnaya Str., Penza, 440026, Russia

E-mail: golpavpnz@yandex.ru

**Abstract.** An automated method for measuring the micro-discharges temperature in the micro-arc oxidation process, allowing measurements to be carried out in real time, is proposed. The design of the measuring transducer, as well as a structural metrological model, taking into account measurement errors is proposed. The possibility of establishing the dependences of the oxide layer micro-hardness on the influencing factors of the micro-arc oxidation process using the Kolmogorov-Johnson-Mehl-Avrami equation by measuring the micro-discharges temperature is shown.

## 1. Introduction

One of the most important tasks of modern science and technology is to ensure the reliability and durability of machine parts, in particular, to protect them from wear and corrosion. For this purpose, micro-arc oxidation – the technology of plasma-chemical hardening of valve metals and alloys, which implies the formation of an oxide layer with high performance characteristics on their surface is currently used [1, 2]. However, due to the simultaneous and joint action of many factors [3] that influence the formation of the oxide layer, finding the optimal technological parameters leading to obtaining coatings of the best quality with minimal expenditure of electricity and time is difficult. To eliminate this problem in [4–6] it was proposed to create a measuring system that allows empirically investigating the influence of the MAO process factors on the properties of the formed coatings in order to obtain mathematical models describing these patterns.

As it is well known, a distinctive feature of micro-arc oxidation are micro-discharges, heating the part surface to high temperatures (about 1500–2000°C) and leading to the “ $\gamma$ -Al<sub>2</sub>O<sub>3</sub> –  $\alpha$ -Al<sub>2</sub>O<sub>3</sub>” phase transition. Therefore, temperature measurement in the discharge channel makes it possible to determine the  $\alpha$ -Al<sub>2</sub>O<sub>3</sub> content in the oxide layer, on which the coating micro-hardness depends.

Traditionally, the temperature in the discharge channel is determined by probe methods according to the volt-ampere characteristic, for which a single or double probe is introduced into the positive column of a glow discharge. However, this method is not applicable to the MAO process, since the pore diameter in which the micro-discharge burns is about 30 nm, and the introduction of any probes into the discharge channel is difficult.

The solution to this problem is the use of non-contact temperature measurement methods based on optical emission spectrometry and pyrometry.

The method of optical emission spectrometry is used to determine the gases composition by measuring the intensity of various spectral lines during gas ignition in a plasma, however, the



temperature in the micro-discharges plasma can also be determined by the luminous intensity of micro-discharges [7–10]. Using this method, the dependences of the electron temperature on the time of the MAO treatment for the magnesium alloy [11] were obtained.

As it is known, the micro-discharges (as well as their brightness) power increases with time depending on the MAO process stage (this also changes their color). Consequently, measuring the micro-discharges brightness makes it possible to determine the temperature in the discharge channel, and knowing this temperature, using the Kolmogorov-Johnson-Mehl-Avrami equation, it is possible to determine the corundum content in the coating.

There are three types of pyrometry: brightness-temperature, color and radiation, in which the laws of Kirchhoff, Wien and Stefan-Boltzmann respectively are used to calculate the heated body the temperature. A common example of brightness pyrometers is a disappearing filament pyrometer, in which the temperature of the sample under study is determined by the coincidence of its luminance brightness with the brightness of the filament, whose temperature is changed. For the MAO process, this method is inapplicable, since the lifetime of a single micro-discharge on the part surface is small (less than half the period of the technological current signal), and because of the flickering effect, it is difficult to choose the desired filament brightness. In addition, the coincidence of the brightness of the filament and the sample under study is determined visually by the operator, while for measuring the micro-discharges brightness in real time, it is necessary to connect the measuring transducer to the microcontroller.

Color pyrometers work on the principle of comparing the energy luminosities of the sample under study at different wavelengths. For this, the investigated thermal radiation alternately passes either through two light filters mounted on a rotating disk, or through two photodetectors closed by these light filters. All this greatly complicates the measuring transducer design and increases its size.

Radiation pyrometers, in contrast to the brightness and color ones, have a simpler design and promising from the point of view of their automation.

To measure the micro-discharges temperature in the MAO process, the authors proposed an automated radiation pyrometric measuring transducer of the micro-discharges temperature of the original design.

## 2. The design of the measuring transducer

The micro-discharge temperature measuring transducer (figure 1) consists of a temperature-to-radiation converter, an optical system, a sensor, a current-to-voltage converter, an amplifier, a low-pass filter, an analog-to-digital converter of the microcontroller and is connected to the computer via the USB interface.

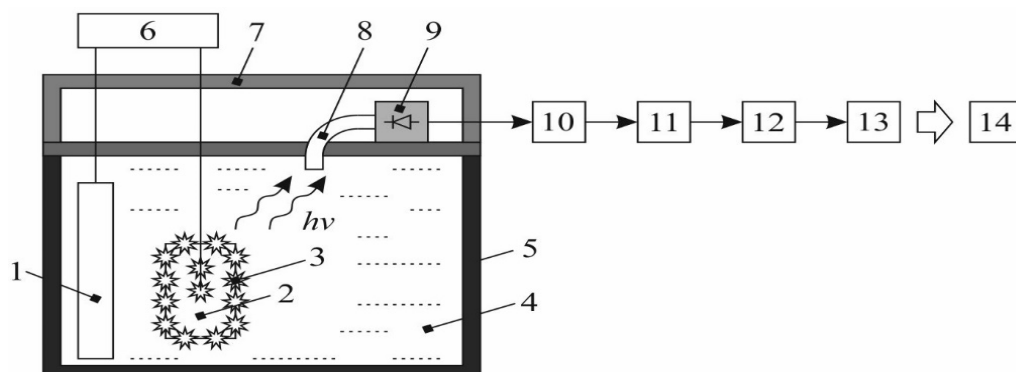


**Figure 1.** The design of the measuring transducer: 1 – cathode; 2 – anode; 3 – micro-discharge; 4 – electrolyte; 5 – cover of galvanic cell; 6 – technological current source; 7 – galvanic cell lid; 8 – optical fiber; 9 – sensor; 10 – current-to-voltage converter; 11 – amplifier; 12 – low-pass filter; 13 – analog-to-digital converter; 14 – computer.

The function of the temperature-to-radiation converter is performed by the sample under study, since with increasing power of micro-discharges on the part surface, the temperature in the discharge channel changes, and accordingly, the brightness and emission spectrum of micro-discharges. The optical system serves to focus the radiation of the sample under study so that the sample projection completely overlaps the sensitive element of the sensor. To do this, you can use a lens, however, it is more expedient to use optical fiber, since the sensor and optical system are located in the galvanic cell lid, and the optical fiber, unlike the lens, is small, not susceptible to fogging and is resistant to corrosive media, in particular, electrolyte.

The sensor can be a pyroelectric sensor, a photoresistor, a phototransistor and a photodiode. In this transducer, a photodiode was chosen as a sensor due to its low inertia and linearity of the light characteristic. Current-to-voltage converter and amplifier are made on operational amplifiers. The low-pass filter is used to separate the useful signal, which is proportional to the integrated intensity of the radiation, from the high-frequency modulating signal caused by the micro-discharges flickering.

### 3. Metrological analysis of the micro-discharges temperature measuring transducer

The structural metrological model of the measuring transducer, presented in figure 2, is made in accordance with the recommendations set out in [12]. In this case, only the first four links of the measuring transducer are considered; the metrological characteristics of the subsequent links depend on the specific circuit design of the device.

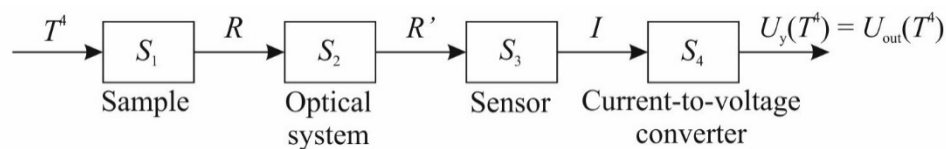


**Figure 2.** Structural metrological model of the measuring transducer:  $T$  – temperature,  $R$  and  $R'$  – input and output radiation intensity of optical system,  $I$  – current,  $U_y(T^4) = U_{out}(T^4)$  – output voltage;  $S_1$ ,  $S_2$ ,  $S_3$ ,  $S_4$  are the sensitivities of the temperature-to-radiation converter, optical system, sensor and current-to-voltage converter respectively.

For the structural metrological model shown in figure 2, the conversion function is:

$$U_y(T^4) = U_{out}(T^4) = T^4 S_1 S_2 S_3 S_4, \quad (1)$$

where  $U_y(T^4) = U_{out}(T^4)$  is the output signal of the micro-discharge temperature measuring transducer,  $T$  is the temperature (the input signal of the measuring transducer is proportional to  $T^4$ ),  $S_1$ ,  $S_2$ ,  $S_3$ ,  $S_4$  are the sensitivities of the temperature-to-radiation converter, optical system, sensor (brightness-to-current converter) and current-to-voltage converter respectively. The sensitivity of the temperature-to-radiation converter is determined according to the Stefan-Boltzmann law for a grey body:

$$S_1 = \frac{R}{T^4} = A_T \sigma, \quad (2)$$

where  $T$  is the true temperature,  $R_{int}$  is the energy luminosity (radiation intensity),  $A_T = 0.2-0.4$  is the integral absorption capacity of aluminium oxide,  $\sigma = 5.66860 \cdot 10^{-8} \text{ W} \cdot \text{m}^{-2} \cdot \text{K}^{-4}$  is the Stefan-Boltzmann constant. Optical system sensitivity

$$S_2 = 1. \quad (3)$$

Integrated sensitivity of the sensor can be found from the expression for the photodiode light characteristic (photocurrent dependences on illuminance) when the photodiode is reverse switched:

$$S_3 = \frac{I}{\Phi} = \frac{q\beta\chi\lambda}{hc} = K, \quad (4)$$

where  $I$  is the photocurrent,  $\Phi$  is the luminous flux,  $q$  is the electron charge,  $\beta$  is the quantum yield of photoionization (the fraction of electron-hole pairs formed by one photon),  $\chi$  is the transfer coefficient, indicating the fraction of electron-hole pairs that did not recombine on the way to p-n-junction,  $\lambda$  is the wavelength of the incident radiation,  $h$  is Planck's constant,  $c$  is the light velocity. Values of the integrated sensitivity of photodiodes are given in reference books.

The sensitivity of the current-to-voltage converter can be found according to Ohm's law using the circuit diagram (figure 3).

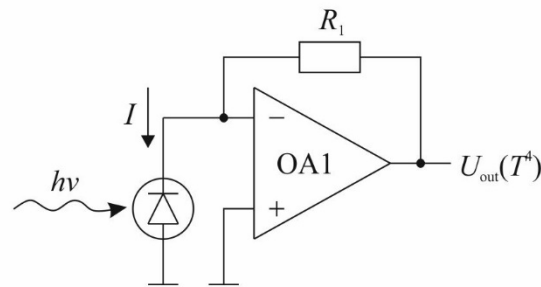


**Figure 3.** The electrical circuit of the current-to-voltage converter.

$$S_4 = \frac{U_{\text{out}}(T^4)}{I} = R_1. \quad (5)$$

Substituting (2)–(5) into (1), we obtain the conversion function of the measuring transducer of microdischarges temperature in the form:

$$U_y(T^4) = U_{\text{out}}(T^4) = T^4 A_T \sigma K R_1. \quad (6)$$

A real measuring transducer has a number of errors, for which a refined structural metrological model has been developed (figure 4).

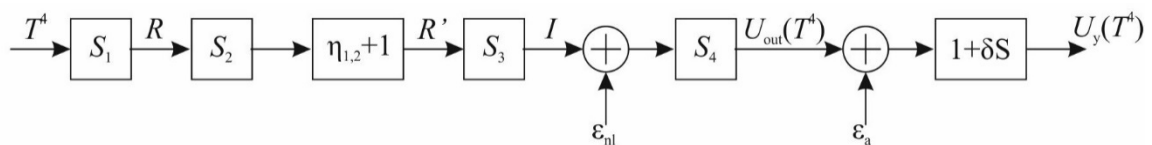


**Figure 4.** Structural metrological model of the measuring transducer, taking into account measurement errors.

In particular, the assumption of linearity of the photodiode light characteristic used in deriving the expression (4) leads to a methodological error, because, first, in the short-wavelength region, the coefficient  $K$  decreases much faster than the formula (4) describes because of an increase in the absorption coefficient; secondly, in the long-wavelength region the photosensitivity decreases, corresponding to the edge of the material own absorption, when the photon energy  $h\nu$  of the incident radiation approaches the band gap of the semiconductor from which the photodiode sensitive element is made. These factors cause the error of nonlinearity  $\varepsilon_{nl}$ . There may be additive  $\varepsilon_a$  and multiplicative  $\delta S$  errors associated, for example, with deviations of the parameters of the operational amplifier from the ideal (input voltage, input bias current, input shift current, etc.). Also, the measurement result can be affected by the methodological matching error  $\eta_{1,2}$  associated with the difference in sensitivity of

the optical system from one (the radiation intensity at the output of the optical system is always less than at the input).

Taking into account the methodological errors, the conversion function of the micro-discharges temperature can be brought to the form:

$$U_y(T^4) = T^4 S_1 S_2 S_3 S_4 (\eta_{1,2} + \delta S + 1) + \varepsilon_{nl} S_4 + \varepsilon_a. \quad (7)$$

The micro-discharges temperature can be obtained from (7) as follows:

$$T = \left( \frac{U_y(T^4) - \varepsilon_{nl} S_4 - \varepsilon_a}{S_1 S_2 S_3 S_4 (\eta_{1,2} + \delta S + 1)} \right)^{\frac{1}{4}}. \quad (8)$$

Knowing the temperature in the micro-discharge channel, according to the Kolmogorov-Johnson-Mehl-Avrami equation, it is possible to determine the proportion of formed corundum ( $\alpha\text{-Al}_2\text{O}_3$ ) in the oxide coating at any time during the MAO treatment, which makes it possible to establish the dependences of the coatings micro-hardness on the influencing factors of the MAO process.

#### 4. Conclusion

Thus, the proposed non-contact automated measurement method allows to determine the micro-discharges temperature in the MAO process in real time. The metrological analysis of the measuring channel allows to take into account and minimize possible errors and guarantee the accuracy of measuring the micro-discharges temperature by the proposed method. The temperature of micro-discharges obtained by the proposed measuring transducer can be used to determine the time dependences of the oxide coatings micro-hardness based on the Kolmogorov-Johnson-Mehl-Avrami equation, and measuring the micro-discharges temperature together with measuring physical quantities describing the influencing factors of the MAO process will allow regularities of the effect of the latter on the micro-hardness of MAO coatings.

#### Acknowledgment

The reported study was funded by RFBR according to the research project No. 19-08-00425.

#### References

- [1] Cheng Y, Wang T, Li S, Cheng Y, Cao J and Xie H 2017 *Elect. Acta.* **225** 47
- [2] Wang K, Koo B-H, Lee C-G, Kim Y-J, Lee S-H and Byon E 2009 *Trans. Nonferrous Met. Soc. China* **19** 866
- [3] Golubkov P E, Pecherskaya E A, Shepeleva Y V, Martynov A V, Zinchenko T O and Artamonov D V 2018 *J. of Phys.: Conf. Ser.* **1124** 081014
- [4] Golubkov P, Pecherskaya E, Karpanin O, Safronov M, Shepeleva J and Bibarsova A. 2019 *Intelligent automated system of controlled synthesis of MAO-coatings* (Moscow: Conference of Open Innovation Association, FRUCT) no 24 pp 96-103
- [5] Golubkov P E, Pecherskaya E A, Karpanin O V, Shepeleva Y V, Zinchenko T O and Artamonov D V 2017 *J. of Phys.: Conf. Ser.* **917** 092021
- [6] Bolshenko A V, Pavlenko A V, Puzin V S and Panenko I N 2014 *Life Sci. J.* **11** 263
- [7] Clyne W, Samuel T and Samuel T 2018 *Int. Mater. Reviews* 1-36
- [8] Hussein R O, Nie X, Northwood D O, Yerokhin A and Matthews A 2010 *J. Phys.: Appl. Phys. D.* **43** 105203
- [9] Wang L, Chen L, Yan Z and Fu W 2010 *Surf. Coat. Technol.* **205** 1651
- [10] Stojadinovic S and Rastko V 2019 *J. Serb. Chem. Soc.* **84** 1
- [11] Darband G B, Aliofkhaezrai M, Hamghalam P and Valizade N 2017 *J. of Magnesium and Alloys* **5** 74
- [12] Pecherskaya E A, Ryabov D V, Shepeleva J V and Pecherskaya R M 2014 *J. of Phys.: Conf. Ser.* **541** 012012